Experiment and Computational Fluid Dynamics (CFD) Simulation of Urea-Based Selective Noncatalytic Reduction (SNCR) in a Pilot-Scale Flow Reactor

Thanh D. B. Nguyen,[†] Young-Il Lim,*[,†] Seong-Joon Kim,[‡] Won-Hyeon Eom,[‡] and Kyung-Seun Yoo[‡]

Laboratory of Functional Analysis of Complex Systems (FACS), Department of Chemical Engineering (RCCT), Hankyong National University, Gyonggi-do, Anseong-si, Jungangno 167, 456-749, Korea, and Department of Environmental Engineering, Kwangwoon University, Seoul, Nowon-gu, Wolgye-dong, 447-1, 139-701, Korea

Received June 19, 2008. Revised Manuscript Received September 9, 2008

A turbulent reacting flow computational fluid dynamics (CFD) model involving a droplet size distribution function in the discrete droplet phase is first built for selective noncatalytic reduction (SNCR) processes using urea solution as a NO_x removal reagent. The model is validated with the experimental data obtained from a pilot-scale urea-based SNCR reactor installed with a 150 kW gas burner. New kinetic parameters of seven chemical reactions for the urea-based NO_x reduction are identified and incorporated into the three-dimensional turbulent flow CFD model. The two-phase droplet model with the non-uniform droplet size is also combined with the CFD model to predict the trajectory of the droplets and to examine the mixing between the flue gas and reagents. The maximum NO reduction efficiency of about 80%, experimentally measured at the reactor outlet, is obtained at 940 °C and a normalized stoichiometric ratio (NSR) = 2.0 under the conditions of 11% excess air and low CO concentration (10−15 ppm). At the reaction temperature of 940 °C, the difference of a maximum of 10% between experiments and simulations of the NO reduction percentage is observed for NSR = 1.0, 1.5, and 2.0. The ammonia slip is overestimated in CFD simulation at low temperatures, especially lower than 900 °C. However, the CFD simulation results above 900 °C show a reasonable agreement with the experimental data of NO_x reduction and ammonia slip as a function of the NSR.

1. Introduction

Selective noncatalytic reduction (SNCR) is a proven cost-effective postcombustion technology for controlling nitrogen oxides (NO_x) from stationary sources, such as power plants, incinerators, and boilers, and there are significant industrial interests in this technology.[1−5] The process is operated by the controlled injection of reducing agents, such as ammonia or urea, into the flue gas without the use of a catalyst. Use of urea (NH_2CONH_2) has been widely accepted as an alternative to ammonia for SNCR of nitric oxides due to its easier and safer handling.[6−10]

While the SNCR processes appear simple, implementation of the process entails a number of challenges. These challenges arise primary because of the relatively narrow temperature window over which the chemicals selectively react with NO_x. In practical systems, the major process parameters that have an effect the performance of SNCR process include (1) reactant mixing, (2) reaction temperature, (3) residence time, (4) the composition of the flue gas (e.g., NO_x, CO, and O_2), and (5) reagent/NO molar ratio (or NSR). Efficiencies increase when all parameters act in concert, so that the reagent is fully mixed with the flue gas at optimum temperatures over a sufficient residence time.[1] Accurate representation of mixing, temperature, and residence time requires coupling between turbulent fluid mechanics, radiative and convective heat transfer, spray droplet dynamics, and gas-phase chemistry.[1]

The rapid industrialization causes severe emissions of air pollutants, and to protect and improve the quality of our environment leads to tightened emission standards. To meet more stringent NO_x emission standards and the need for low-cost control technologies, innovative design solutions by improved computational tools are needed for SNCR design and optimization.[1,11−13] Computational fluid dynamics (CFD) is one tool available to aid the design of SNCR in the most efficient

* To whom correspondence should be addressed. Telephone: +82-31-670-5207. Fax: +82-31-670-5445. E-mail: limyi@hknu.ac.kr.

[†] Hankyong National University.

[‡] Kwangwoon University.

(1) Cremer, M. A.; Montgomery, C. J.; Wang, D. H.; Heap, M. P.; Chen, J.-Y. *Proc. Combust. Inst.* **2000**, *28*, 2427–2434.

(2) Wendt, J. O. L.; Linak, W. P.; Groff, P. W.; Srivastava, R. K. *AIChE J.* **2001**, *47* (11), 2603–2617.

(3) Muzio, L. J.; Quartucy, G. C.; Cichanowicz, J. E. *Int. J. Environ. Pollut.* **2002**, *17* (1/2), 4–30.

(4) Himes, R.; Hubbard, D.; West, Z.; Stallings, J. Joint Electric Power Research Institute (EPRI)/Environmental Protection Agency (EPA) Symposium on Stationary NO_x Control, Kansas City, MO, 1995.

(5) Tayyeb Javed, M.; Irfan, N.; Gibbs, B. M. *J. Environ. Manage.* **2007**, *83* (3), 251–289.

(6) Sun, W. H.; Stamakis, P.; Hofman, J. E. *ACS Sym. Ser.* **1993**, *38*, 734–739.

(7) Lee, J. B.; Kim, D. D. *J. Chem. Eng. Jpn.* **1996**, *29*, 620–626.

(8) Muzio, L. J.; Arand, J. K.; Teixeira, D. P. The 16th International Symposium on Combustion, The Combustion Institute, Pittsburgh, PA, 1997; pp 199−208.

(9) Alzueta, M. U.; Bilbao, R.; Millera, A.; Oliva, M.; Ibanez, J. C. *Energy Fuel* **1998**, *12*, 1001–1007.

(10) Gentemann, A. M. G.; Caton, J. A. Proceedings of the 21st German Flame Day Conference, Combustion and Furnaces, University of Cottbus, Cottbus, Germany, 2003; pp 497−502.

(11) Baukal, C. E.; Hayes, R.; Grant, M.; Singh, P.; Foote, D. *Environ. Prog.* **2004**, *23* (1), 19–28.

10.1021/ef8004652 CCC: $40.75
Published on Web 10/29/2008

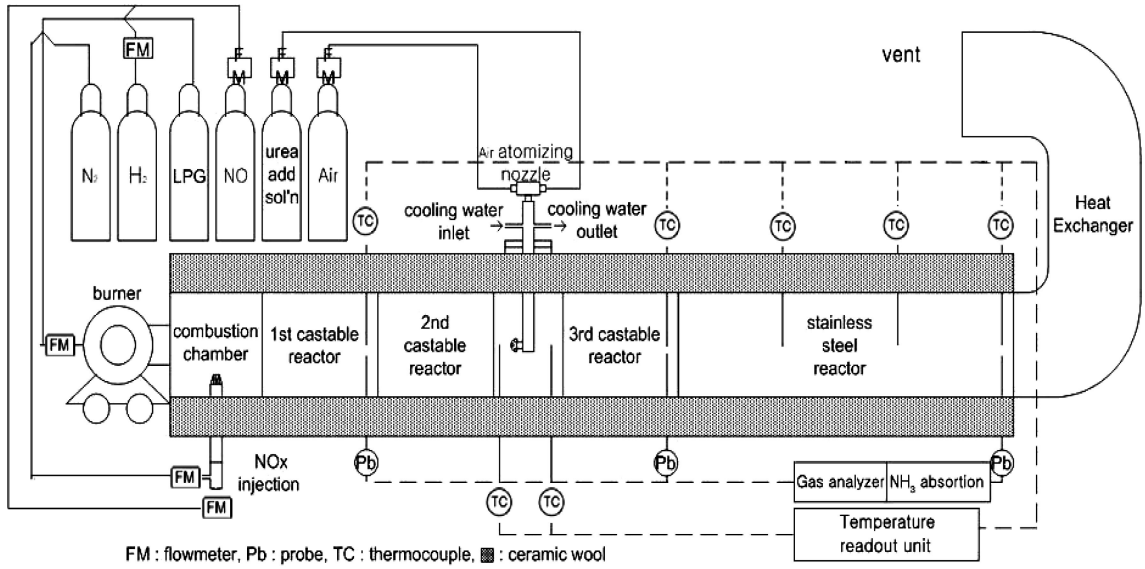

Figure 1. Pilot-scale experimental setup equipped with a gas burner.

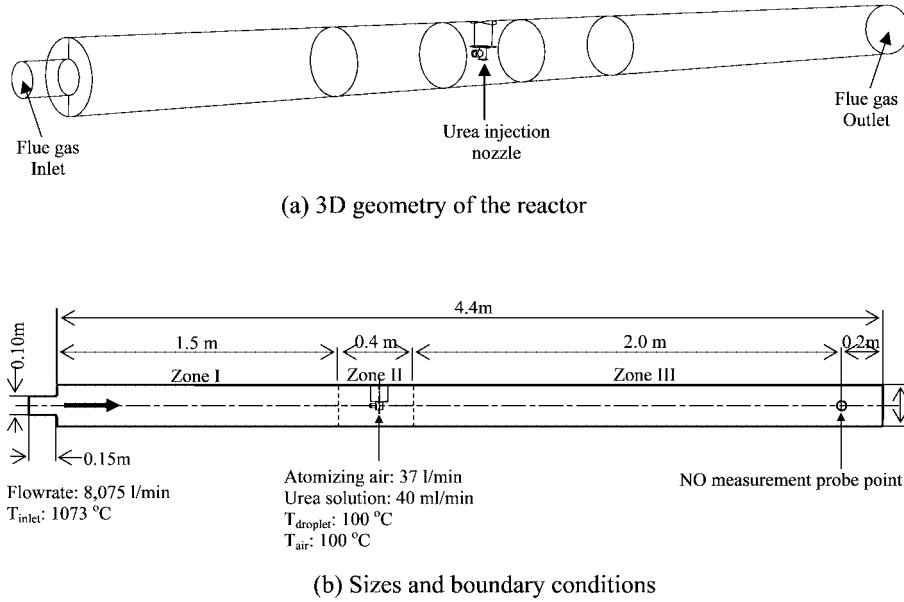

Figure 2. Geometry and boundary conditions of NO_x reduction reactor in CFD simulation.

and cost-effective way.[14] CFD modeling with the turbulent reacting flow model can provide several advantages for the design of the SNCR system. These include an improved understanding of complex physical and chemical behaviors, such as flue gas patterns, gas velocities, pressure drop, temperature and species concentration profiles, optimal reagent injection locations, and the effect of the normalized stoichiometric ratio (NSR $= 2n_{urea}/n_{NO}$, where n_{urea} is moles of urea in the urea solution injected into the reactor and n_{NO} is moles of NO in the flue gas) for NO_x reduction.

Coupling turbulence and heat transfer with the fully detailed chemistry[15] is prohibitive from the standpoint of both CPU time and memory.[1,16−18] Therefore, CFD modeling with reduced kinetic models are widely adopted.[1,16,17,19] Reduced kinetic models for NO_x reduction have been reported by several authors.[1,7,16,20,21] Brouwer et al.[16] developed and implemented

(12) Heggemann, M.; Wintergerste, T. *Chem. Eng. Technol.* **2004**, *27* (9), 982–987.
(13) Chacon, J.; Sala, J. M.; Blanco, J. M. *Energy Fuel* **2007**, *21*, 42–58.
(14) Han, X.; Wei, X.; Schnell, U.; Hein, K. R. G. *Combust. Flame* **2003**, *132* (3), 374–386.
(15) Miller, J. A.; Bowman, C. T. *Prog. Energy Combust. Sci.* **1989**, *15*, 287–338.
(16) Brouwer, J.; Heap, M. P.; Pershing, D. W.; Smith, P. J. The 26th International Symposium on Combustion, The Combustion Institute, Naples, Italy, 1996; pp 2117−2124.
(17) Montgomery, C. J.; Swensen, D. A.; Harding, T. V.; Cremer, M. A.; Bockelie, M. J. *Adv. Eng. Software* **2002**, *33* (2), 59–70.
(18) Skjoth-Rasmussen, M. S.; Holm-Christensen, O.; Ostberg, M.; Christensen, T. S.; Johannessen, T.; Jensen, A. D.; Glarborg, P.; Livbjerg, H. *Comput. Chem. Eng.* **2004**, *28*, 2351–2361.
(19) Department of Energy (DOE) topical report. Engineering development of coal-fired high performance power systems, phase II: Selective non-catalytic reduction system development. Report number DOE/PC/95144-T4, United Technologies Research Center, East Hartford, CT, 1997; http://www.osti.gov/bridge.
(20) Duo, W.; Dam-Johansen, K.; Ostergaard, K. *Can. J. Chem. Eng.* **1992**, *70*, 1014–1020.
(21) Ostberg, M.; Dam-Johansen, K. *Chem. Eng. Sci.* **1994**, *49*, 1897–1904.

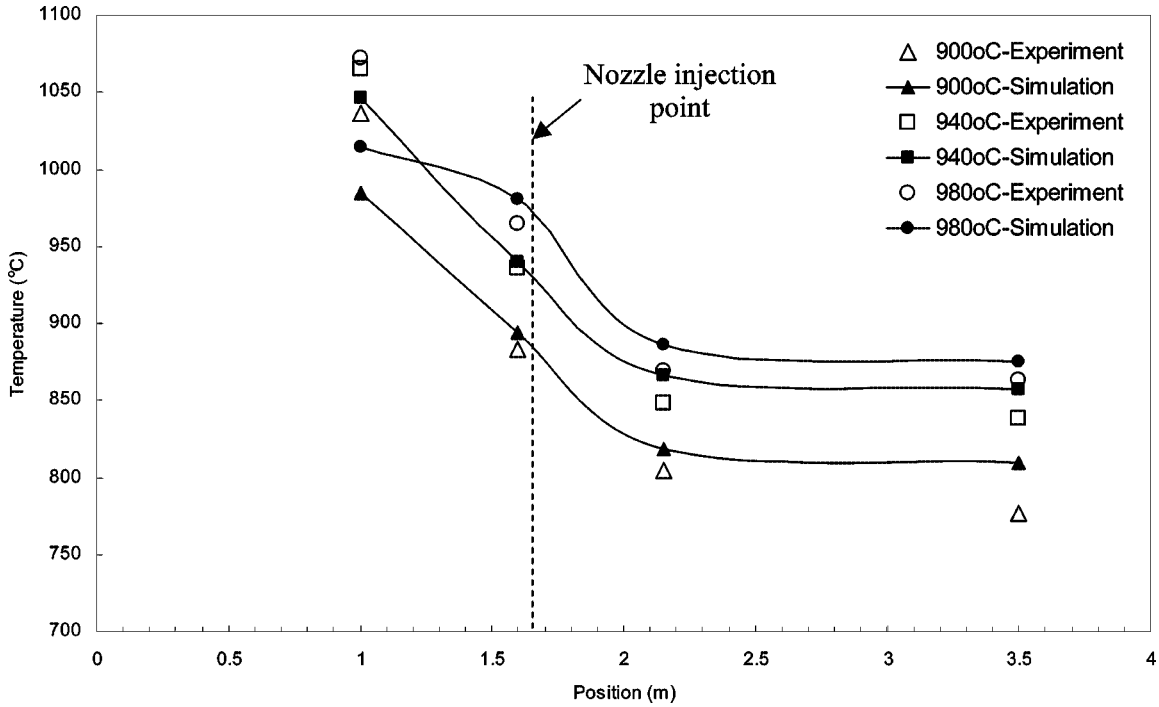

Figure 3. Temperature profiles along the reactor of experiments and simulations.

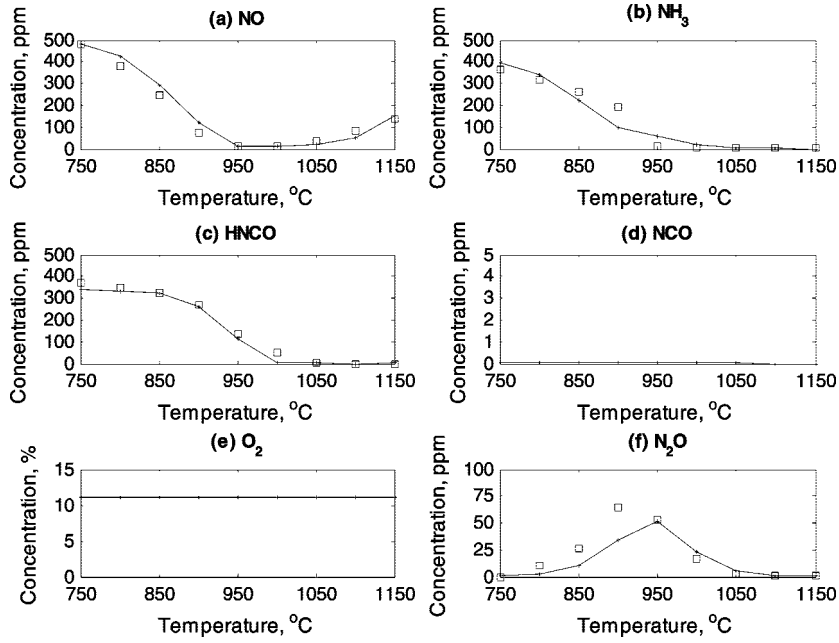

Figure 4. Concentration profiles of six main species with temperature at $[NO]_{initial}$ = 500 ppm, NSR = 1.5, and τ = 0.1 s (−×−, the reduced model; □, the full model).

a seven-step global kinetic mechanism (seven reactions with six species) for SNCR chemistry into a three-dimensional CFD simulation.

In this study, the pilot-scale experimental results using urea solution are compared to the CFD simulation results on temperature and NO and NH_3 concentrations. The seven chemical reactions[16] are used to predict the concentration of NO, NH_3, and N_2O in combination with a CFD code, Fluent (Fluent, Inc., Lebanon, NH).[13,19]

The present work aims to (1) develop a three-dimensional CFD-based reacting model using Fluent to predict flow field, temperature distribution along the reactor, and species concentrations at the exit (e.g., NO and NH_3), (2) incorporate the kinetic mechanism (seven reactions with six species) for NO reduction by urea−water solution with the CFD model, and (3) validate the turbulent reacting flow CFD model with a pilot-scale flow reactor experimental data for its practical applications to full-scale SNCR processes.

The remainder of the paper is organized as follows: Section 2 explains the experimental setup and procedure. Section 3 presents the CFD model with the kinetics proposed in this study, which are described in detail in the Appendix. Experimental data are compared to the CFD simulation results and are analyzed in Section 4. The conclusions are finally presented in Section 5.

2. Experimental Section

The NO reduction experiments by the urea−water solution are carried out in a pilot-scale flow reactor. The experimental setup is

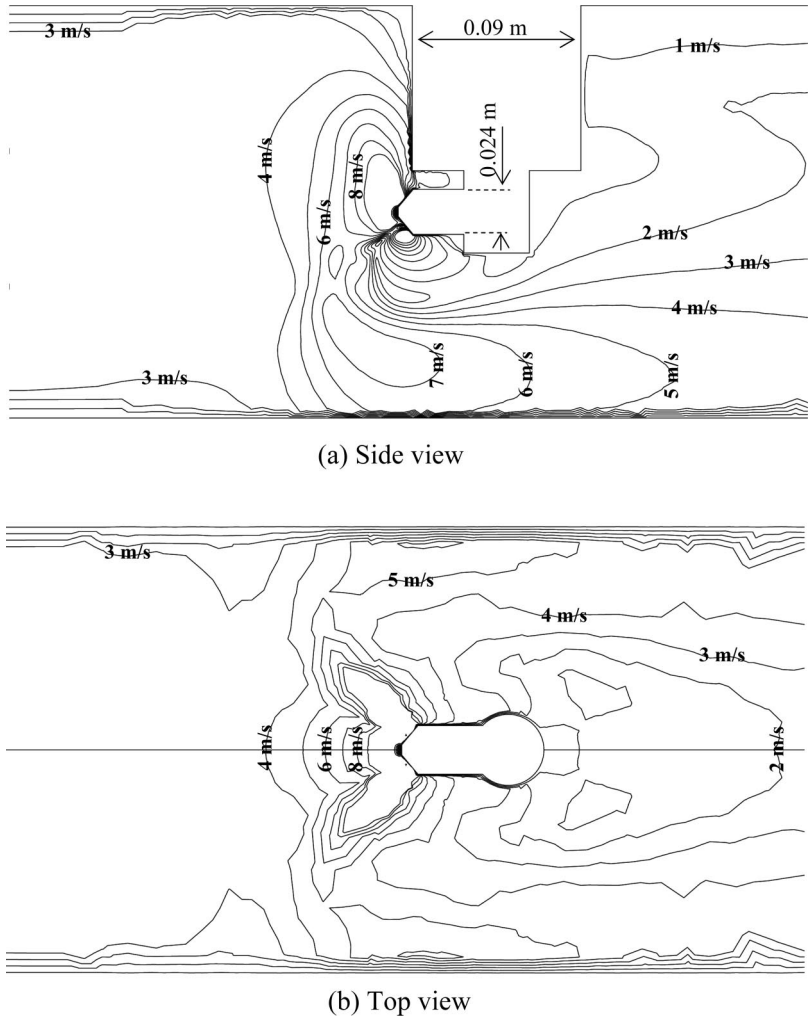

Figure 5. Contours of velocity near the nozzle in the case of T_R = 940 °C.

illustrated in Figure 1.[22] The reaction temperature is controlled by a cylindrical gas-fired burner installed at the reactor inlet. The gas burner has a heating rate of 50−150 kW.

The combustion chamber (see Figure 1) is made of castable HSC 18 [inner diameter (ID) = 0.22 m, length (L) = 0.5 m, and thickness = 0.1 m]. The high-temperature zone (or from the first to the third castable reactor; ID = 0.22 m, L = 2.5 m) next to the combustion chamber is also made of castable HSC 18. The low-temperature reactor zone or the stainless-steel reactor (ID = 0.22 m, L = 2.0 m) follows the high-temperature zone and is made of SUS 304. The burner and the reactor walls are insulated with 0.15 m thick ceramic wool to achieve a constant temperature gradient by preventing heat loss to the surroundings. Figure 2 shows a three-dimensional schematic in scale of the pilot-scale reactor. The mean temperature decreasing rate around the NO_x reduction zone (zone II in Figure 2b) is about 55−75 °C/m (see Figure 3). The outlet gases from the reactor are cooled in a heat exchanger before being exhausted to the atmosphere.

Uniform mixing of fuel gases with the reagent (urea−water solution) plays an important role in improving NO_x reduction, and the injection nozzle is a key component.[5] The droplet size, its distribution, and injection velocity are main factors in selecting suitable injectors. In the present study, urea−water solution is injected through a water-cooled atomizing nozzle of an injection angle of 70° and 6 holes (ID = 1.016 mm). This nozzle releases the mean droplet size of 36 μm at the injection pressure of 3 atm.

The temperatures are measured using seven thermocouples, as shown in Figure 1. The first temperature is measured using a R-type thermocouple, and others are measured by K-type thermocouples. The reaction temperature (T_R) is measured by the second thermocouple located 5 cm in front of the nozzle. The total flow rate through the reactor is maintained at about 8000 L/min (lpm) in the case of T_R = 940 °C. The inlet concentration of NO to the reactor is controlled at about 400 ppm by regulating the NO (99.5% pure NO) flowrate. The excess oxygen in the flue gas maintains the range of 10−12 vol %. Air (about 37 lpm) is introduced at 3 atm into the nozzle for atomizing the urea solution of 5 wt % and 40 mL/min. The weight concentration of the urea solution (5 wt %) was experimentally confirmed as an optimum value to maximize NO_x reduction.[22]

NSR is varied from 1.0 to 2.0. NO_x is measured from the sampling probe located at 2.8 m behind the nozzle injection point. The concentration of NO_x is measured using the NO/CO analyzer. NH_3 is also measured by the NH_3 electrode. Since the fuel gas is almost perfectly combusted with 11% excess air, CO (carbon monoxide) measured is about 10−15 ppm at the inlet of the reactor.

3. Modeling and Simulation

A turbulent reacting flow CFD model involving the discrete droplet phase is developed for the pilot-scale urea-based SNCR reactor. The pilot-scale flow reactor is fully represented by a three-dimensional (3D) symmetric geometry (see Figure 2a). Figure 2b shows the symmetric geometry and boundary conditions at the reactor inlet and outlet and the nozzle inlet.

The wall boundary temperature is adjusted in an iterative way to achieve the temperature quench rate, which was measured in the experiments. Figure 3 compares the temperature profiles along the reactor length between experiments and simulations at three

(22) Park, S. Y.; Yoo, K. S.; Lee, J. K.; Park, Y. K. *Korean Chem. Eng. Res.* **2006**, *44* (5), 540–546.

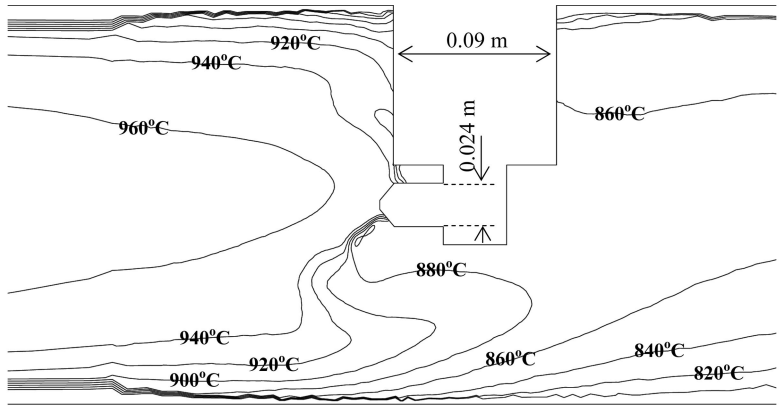

(a) Side view

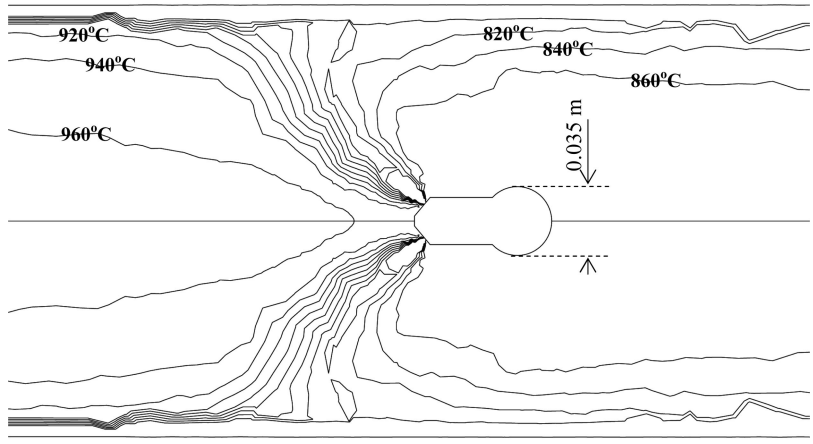

(b) Top view

Figure 6. Contours of temperature near the nozzle in the case of T_R = 940 °C.

different reaction temperatures (900, 940, and 980 °C). In the case of T_R = 940 °C, the mean temperature decreasing rate along the reactor length obtained from the simulation is 76 °C/m, which is the same as that of the experiment. The temperature decreasing rate with the position just behind the nozzle is large because of the urea solution injection from the nozzle, as shown in Figure 3. The linear functions of the wall boundary temperature are given in Appendix A2. The three-dimensional mesh structure and boundary conditions are explained in detail in Appendices A1 and A2, respectively.

The seven-step global reaction[16] is used, which considers NH_3 and HNCO reaction paths with N_2O reactions (see Table A7 for reaction kinetics). The kinetic parameters of Brouwer et al.[16] are modified to better fit the results from the full chemical kinetics mechanism,[15] ignoring the effect of CO and considering the excess oxygen of 11%, since this pilot-scale SNCR reactor, similar to an incinerator, is operated at those conditions.

In the SNCR kinetics, thermal decomposition of urea to NH_3 and HNCO plays a major role for temperatures below 850 °C, whereas for temperatures above 850 °C, the oxidation becomes important.[23] Since the temperature range considered in this study is from 850 to 1010 °C, the reduced SNCR kinetic mechanism assumes instantaneous reagent breakdown into ammonia (NH_3) and isocyanic acid (HNCO) in the gas phase.[16]

The reaction mechanism compares well to the fully detailed chemical kinetic mechanism,[15] as indicated in Figure 4 for isothermal and homogeneous conditions at various reaction temperatures (T_R). These kinetic parameters (see Table A7) are estimated from the minimization of the total square error of NO, NH_3, HNCO, and N_2O concentrations between the full model and the reduced one. The results obtained from the full model[15] are indicated in squares in parts a−c and f of Figure 4. The NO concentration increases with an increase of the temperature over 1000 °C, because the NO formation rate increases over that temperature.

The three-dimensional CFD-based turbulent reacting flow model is developed. This model involves governing transport equations of chemical species (see Appendix A3), turbulent flow modeling (see Appendix A4), an eddy-dissipation-concept (EDC) model for the chemical reaction modeling in the turbulent flow (see Appendix A5), and governing equations of the droplet phase (see Appendix A6). The droplet size distribution function (Rosin−Rammler probability density function[24]) is used, with the mean droplet size ($d_{p,mean}$) of 36 μm and the droplet size range of $1 \le d_p \le 100$ μm.

Several difficulties are encountered in coupling kinetics with a CFD code.[19] The direct use of the full reaction mechanism in CFD modeling of practical problems is usually prohibitive because of the large computing time.[14] It is necessary to supply realistic boundary conditions (temperature, velocity, and concentrations of species) at the inlets of the simulated domain.[19] It has also been experienced in this work that the convergence was not guaranteed, if unrealistic boundary conditions were given. In Tables A1−A6 of the Appendix, the boundary conditions are given in the case of T_R = 940 °C for reactor inlet gas, atomizing air, and urea solution from the nozzle for NSR = 1.0, 1.5, and 2.0.

The contours of velocity near the nozzle are shown in the case of T_R = 940 °C in Figure 5. The mean bulk velocity (v_{mean})

(23) Gentemann, A. M. G.; Caton, J. A. Proceedings of the 2nd Joint Meeting of the United States Sections of the Combustion Institute, Oakland, CA, 2001; pp 1−7.

(24) Yoon, S. S.; Kim, H. Y.; Hewson, J. C. *Fire Saf. J.* **2007**, *42*, 393–406.

Table 1. Comparison of NO_x Reduction Percentage between Experiment and Simulation at Three Different Temperatures and NSRs

temperature (°C)	NSR	experiment (%)	simulation (%)	difference (%)[a]
900	1.0	45 ± 3	28	17
889	1.5	14 ± 2	44	30
900	2.0	61 ± 3	55	6
940	1.0	56 ± 3	51	5
940	1.5	73 ± 4	70	3
940	2.0	81 ± 4	91	10
980	1.0	53 ± 3	50	3
976	1.5	69 ± 4	67	2
980	2.0	71 ± 4	84	13

[a] Difference = |experimental result − simulation result|.

experimentally measured is about 6.3 m/s in the case of T_R = 970 °C.[22] The simulation result of the mean bulk velocity (6 m/s) at T_R = 940 °C agrees well with that of the experiment. In Figure 5a seen at the side of the nozzle, the flow velocity is strongly perturbed in front of the nozzle and a low-velocity region is observed behind the nozzle. The symmetric velocity contour is shown in Figure 5b seen at the top of the nozzle.

The contours of temperature in the case of T_R = 940 °C near the nozzle are shown in Figure 6 seen at the side and the top. The temperature profile is distributed and nonhomogeneous near the nozzle. Thus, the reaction temperature (T_R) indicating the temperature at 5 cm in front of the nozzle is not an exact reaction temperature but is considered as a representative one. The residence time for NO_x reduction is estimated to be about 0.05 s on the basis of the mean residence time of droplets at T_R = 940 °C (see Figure A3), while the residence time of less than 0.1 s is required for sufficient NO_x reduction at T_R = 950 °C.[21]

4. Results and Discussion

In this section, experiment and simulation results of the NO and NH_3 concentrations at the reactor outlet are compared and analyzed. A total of 15 experiments are performed in the temperature range of 850 ≤ T_R ≤ 1010 °C and at NSR = 1.0, 1.5, and 2.0. At each reaction temperature and NSR, three separate experiments are carried out for verification. Table 1 shows the NO reduction percentage obtained from experiments and simulations at the three temperatures and the three NSRs. Experimental data represent the mean values with the 5% error bound of the three repeated experiments at each condition.

The turbulent reacting flow CFD model is applied for just nine cases at three different reaction temperatures T_R = 900, 940, and 980 °C, with NSR = 1.0, 1.5, and 2.0. The CFD model is validated by comparing it to the experimental data for the nine cases. It is noted that the turbulent reacting flow CFD model proposed in this study is focused on the interesting temperature range, 900 ≤ T_R ≤ 1000 °C.

4.1. NO_x Reduction. For full-scale applications, NO reductions of approximately 30−60% have been achieved, while bench-scale testing often achieves greater reductions.[2,4] Urea alone in water has a high NO_x reduction efficiency at roughly 930−1040 °C.[5]

In Table 1, the experimental and CFD simulation results for the nine cases of NO_x reduction are compared. In this pilot-scale flow reactor, the optimum temperature is about 940 °C. NO_x reduction of 73% is achieved at NSR = 1.5, and NO_x reduction reaches about 80% at NSR = 2.0 for the optimum temperature (T_R = 940 °C).

Figure 7 shows the NO_x reduction percentage with respect to the reaction temperature (T_R) at the three different NSRs. The error bars of the measured temperature and NO concentration are shown in Figure 7. For the temperature, the K-type thermocouple located at 5 cm in front of the nozzle is guaranteed within ±5 °C by the manufacturer. The error bound of NO measurement is ±5%, including the analyzer instrumental error (±1%) and the other errors (about ±4%), which are approximately obtained by the three repeated tests performed under the same experimental conditions.

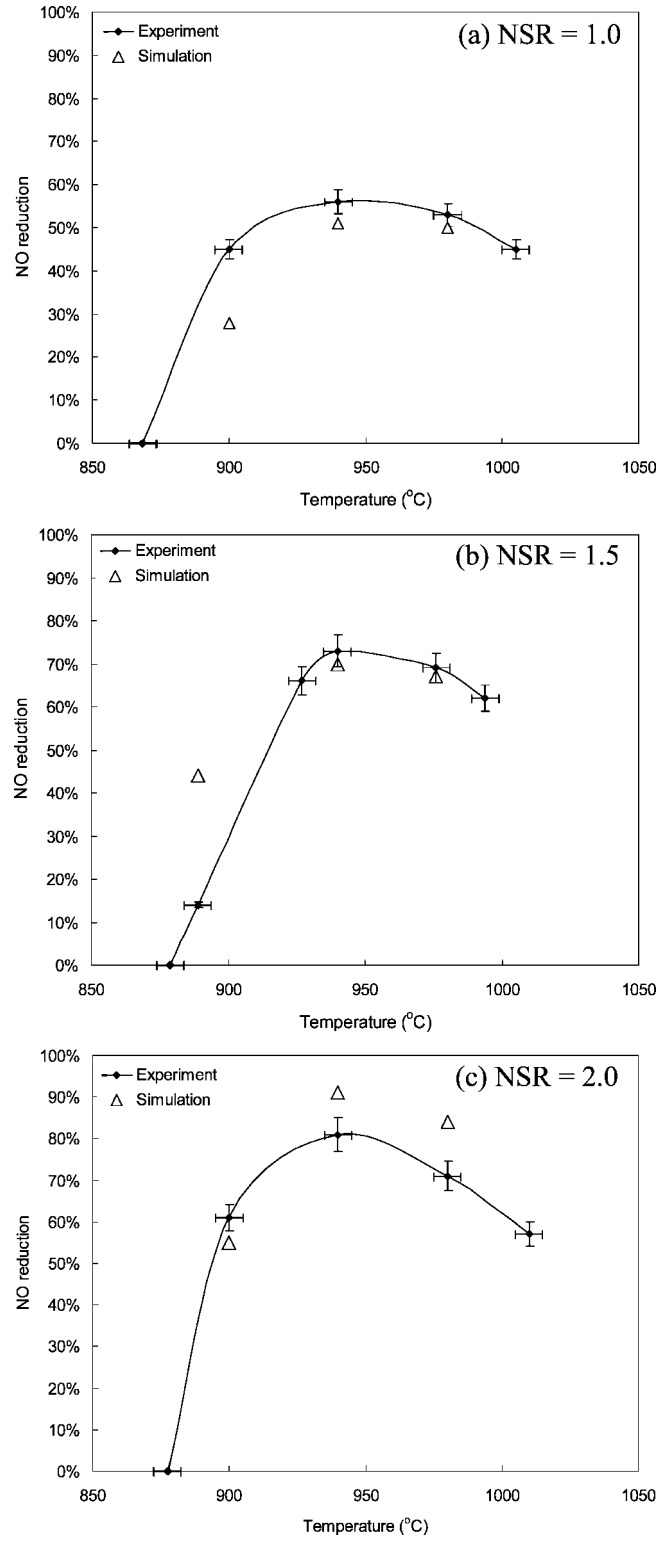

Figure 7. NO reduction percentage with respect to temperature.

The predictions show reasonable agreement with experimental data, except for the two cases (T = 900 °C/NSR = 1.0 and T = 889 °C/NSR = 1.5) that show above 15% difference between the experiment and simulation. The NO reduction is very low in the experimental results at T_R = 889 °C and NSR = 1.5,

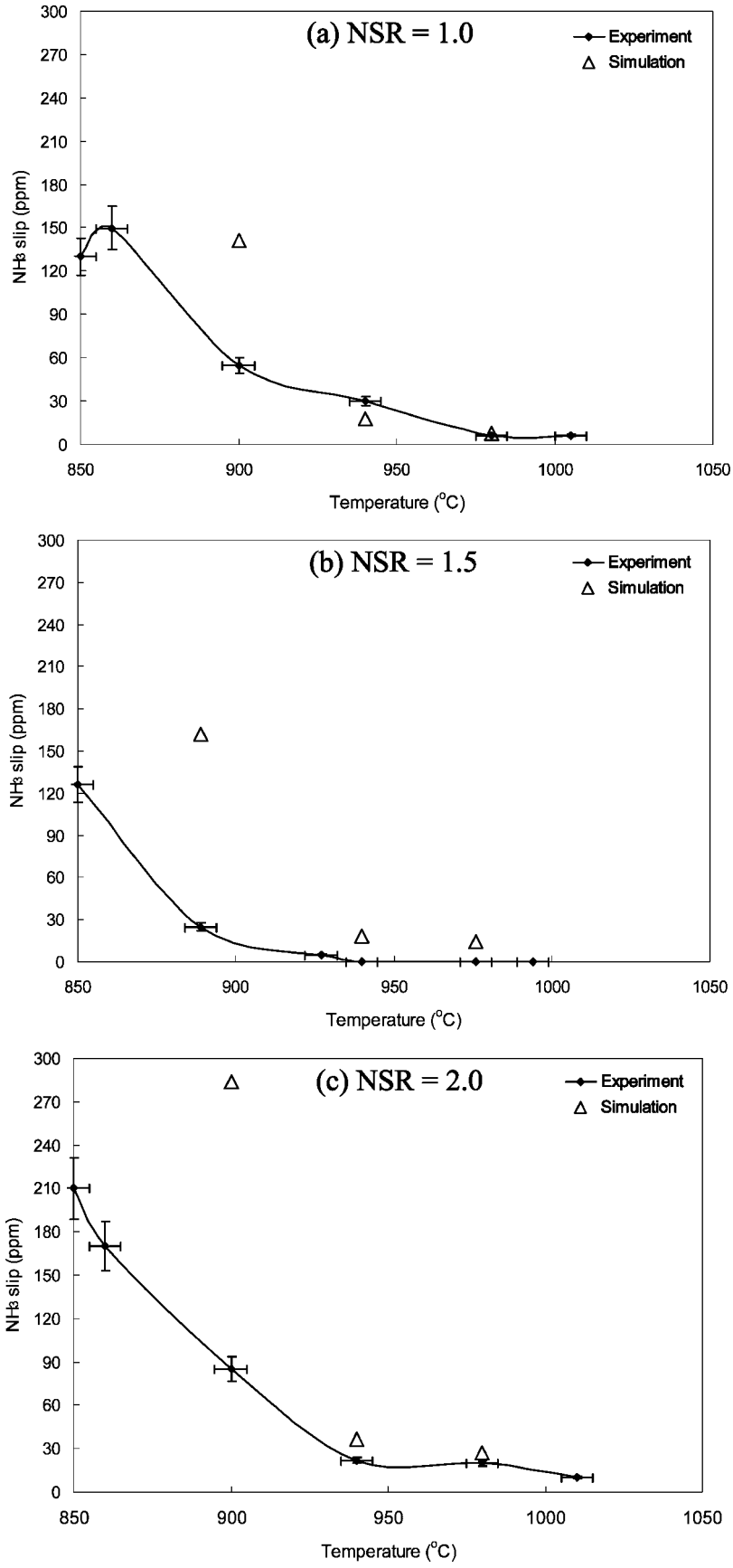

Figure 8. NH_3 slip with respect to temperature.

while the simulation results predict the general trend in the SNCR operation (see Figure 7b). In the pilot-scale experiments with 150 kW combustor, the low NO reduction is observed below 900 °C, as shown in Figure 7. That may result from non-uniform temperature distribution over the reaction area and nonperfect mixing near the nozzle.

As stated in Brouwer et al.,[16] the reduced chemistry with seven reactions does not work well over a wide temperature

window, because the applicable range of SNCR is limited to a narrow temperature window. The kinetics proposed in this study does not cover the wide range of temperatures, especially, below 900 °C, although it agrees well with the fully detailed kinetic mechanism[15] (see Figure 4). However, the simulation results show the same trend as the experimental data and predict well for seven of nine cases (see Figure 7 and Table 1).

4.2. NH_3 Slip. Minimum unreacted NH_3 from SNCR processes is desirable from an environmental as well as a combustor standpoint.[5] With the SNCR process, the subject of NH_3 slip is quite complicated because it depends upon the interaction of numerous factors, such as the composition of flue gas, the effectiveness of mixing NH_3 with flue gas, reaction time, and temperature.[5] Nevertheless, it is clear that unreacted ammonia is dependent upon the NSR and the reaction temperature because they are the main operating parameters.

The results of NH_3 slip obtained from the CFD simulation and experiment are shown in Figure 8, including the error bound of experimental results. The ammonia concentration has a bigger error bound of ±10% than NO because of the larger analyzer instrumental error (±5%). The error bars with ±5 °C of temperature and ±10% of the NH_3 concentration are shown in Figure 8.

At low temperatures (below 900 °C), big differences between the experimental data and the simulation results are observed for ammonia slip. Overestimation of ammonia slip increases as NSR increases at these low temperatures, because there is a lot of unreacted ammonia that remains. According to Brouwer et al.,[16] ammonia slip is also overestimated at lower temperatures (less than 1000 °C) using the same reduced reaction mechanism. However, the simulation results of the ammonia slip show a similar tendency to the experiments and agree with experimental measurements at T_R = 940 and 980 °C (see Figure 8).

5. Conclusions

Experiments are carried out in the pilot-scale flow reactor installed with a 150 kW gas burner for identification of urea-based SNCR performance with respect to temperature and NSR. The three-dimensional turbulent reacting flow CFD model is constructed and validated with the experimental data obtained from the pilot-scale SNCR process. The two-phase droplet model with the non-uniform droplet size is developed to identify the trajectory of droplets.

The seven-step global reaction mechanism for NO_x reduction by the urea−water solution is incorporated with the CFD simulation to predict NO_x reduction, ammonia slip, and the optimum reaction temperature. The mixing near the nozzle between reactants is examined by using the two-phase CFD model of turbulent reacting flow.

The CFD simulation results show a satisfactory agreement with the experimental data of NO_x reduction and ammonia slip as a function of the temperature and the NSR. However, the CFD model with seven chemical reactions used in this study does not work well below 900 °C in predicting the experimental data of this pilot-scale SNCR process.

Acknowledgment. This study is supported by the Korea Ministry of Environment as "The Eco-technopia 21 Project".

Appendix

A1. Mesh Construction. A mesh generator in a CFD code divides the computational domain of the whole reactor into cells, upon which conservation equations for mass, momentum, and energy are solved and velocity, temperature, and species concentrations are computed at each cell.[5]The pilot-scale flow reactor (see Figure 2; 0.22 m ID × 4.4 m *L*) is divided into three computational zones in the symmetric third dimension (3D): (1) reactor inlet zone, where the flue gas enters into the reactor; (2) nozzle inlet zone, where the reagent urea is injected into the reactor and the reaction takes place; and (3) outlet zone of the exit gas. The grid is generated using Gambit 2.3.16 (Fluent, Inc., Lebanon, NH). The mesh configuration near the nozzle is shown in Figure A1. The six holes of 1 mm ID are located on the nozzle tip with the injection angle of 70° (see also Figure A3). The meshes are generated using volume meshing with the Hex (Cooper scheme for zones I and III) and the Tet/Hybrid (TGrid scheme for zone II). The total number of meshes is about 600 000 for one symmetric part of the 3D geometry, of which CFD results (i.e., temperature) show a converged value according to the number of meshes.Once the discretization of the geometry is completed, the mesh is to be totally exported into the main processor, where the boundary conditions are usually applied to complete the numerical model.

A2. Boundary Conditions. The flue gas (350−380 ppm NO, 10 vol % O_2, and balanced N_2) enters into the reactor inlet at a flow rate of about 8000 lpm at the inlet temperature, T_{inlet} = 1075 °C, in the case of T_R = 940 °C. The nozzle atomizing air has a flow rate of 37 lpm at standard temperature and pressure (STP; 0 °C and 1 atm). The flow rate of the urea−water solution is 40 mL/min at 20 °C and 3 atm (see Figure 2b). The liquefied petroleum gas (LPG) used in experiments is approximated to be 50% C_3H_8 and 50% C_4H_{10} and is considered to be bunt completely with the excess air to form CO_2 and water vapor. It is supposed that LPG enters into the combustor at 0 °C and 1 atm, the excess air is mixed with LPG at 20 °C and 1 atm, and pure N_2 with pure NO is injected at 20 °C and 1.5 atm into the reactor. The urea−water solution is pressurized by the nitrogen gas at 3 atm. The atomizing air is also released from the nozzle at 3 atm.The excess O_2 percentage can be calculated from the following stoichiometric balance:

$$C_{3.5}H_9 + (5.75O_2 + 21.63N_2)^a + (xO_2 + 3.762xN_2)^b + (yN_2)^c + (zO_2 + 3.762zN_2)^d = 3.5CO_2 + 4.5H_2O + 21.63N_2 + (xO_2 + 3.762xN_2) + yN_2 + (zO_2 + 3.762zN_2) \quad \text{(A2.1)}$$

where *a* is the required air for the complete combustion, *b* is the excess air from the burner, *c* is the pure N_2 to carry the pure NO at the reactor inlet, and *d* is the atomized air to be injected from the nozzle. Here, *x* is the ratio of excess O_2/LPG; *y* is the amount of pure N_2 in NO injected flow; and *z* is the amount of O_2 in atomizing air.In the reaction A2.1, all of the species are considered as the ideal gases at STP. If the volume flow rate of LPG used is *V* (lpm), the excess O_2 can be calculated as follows:

$$\%O_2\ (\text{excess}) = \frac{(x+z)\times 100}{V(3.5+21.63)+x(1+3.762)+y+z(1+3.762)} \quad \text{(A2.2)}$$

The detail mass and molar flow rates of the reactor and nozzle inlets are given in Tables A1−A6 for the case of T_R = 940 °C and NSR = 1.0, 1.5, and 2.0.Tables A1 and A2 specify flow rates of each species at the reactor inlet at STP. The total flow rate at this condition is about 1700 L/min. In Table A3, the total flow rate of atomizing air is about 37 lpm. Tables A4−A6 show the flow rates of the urea−water solution in the case of T_R = 940 °C and NSR = 1.0, 1.5, and 2.0. Those boundary conditions are based on the experimental conditions that were carried out in the pilot-

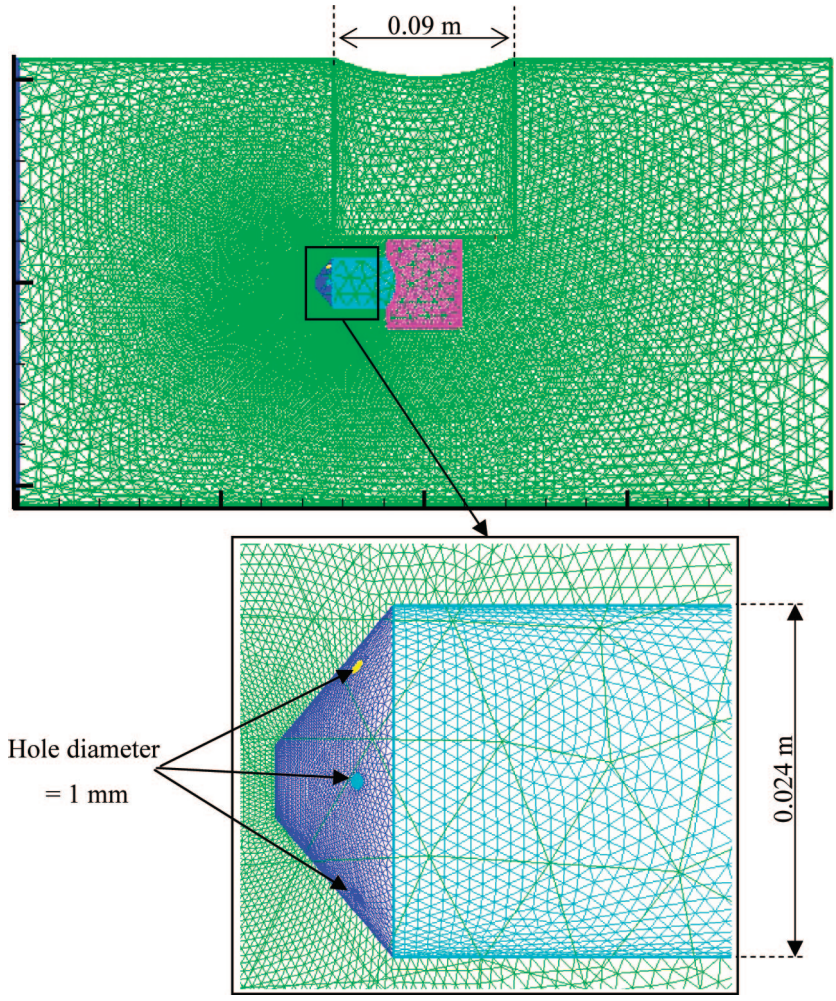

Figure A1. Mesh configuration near the nozzle and hole positions.

Table A1. Boundary Conditions at the Reactor Inlet at NSR = 1.0 and 2.0 in the Case of T_R = 940 °C

species	L/min	mol/min	mol fraction	g/min	mass fraction	kg/s
CO_2	103.01	4.60	0.060	202.33	0.093	0.003
H_2O	132.44	5.91	0.078	106.42	0.049	0.002
O_2	169.48	7.57	0.099	242.11	0.111	0.004
N_2	1302.08	58.13	0.763	1627.60	0.747	0.027
NO	0.60	2.66×10^{-2}	3.49×10^{-4}	0.80	3.67×10^{-4}	1.33×10^{-5}
total	1707.59	76.23	1	2179.25	1	0.036

Table A2. Boundary Conditions at the Reactor Inlet at NSR = 1.5 in the Case of T_R = 940 °C

species	L/min	mol/min	mol fraction	g/min	mass fraction	kg/s
CO_2	92.75	4.14	0.060	182.19	0.093	0.003
H_2O	119.25	5.32	0.077	95.83	0.049	0.002
O_2	152.47	6.81	0.099	217.81	0.111	0.004
N_2	1174.71	52.44	0.763	1468.39	0.747	0.024
NO	0.59	2.62×10^{-2}	3.80×10^{-4}	0.78	3.99×10^{-4}	1.31×10^{-5}
total	1539.77	68.74	1	1965.00	1	0.033

Table A3. Boundary Conditions for Atomizing Air at NSR = 1.0, 1.5, and 2.0 in the Case of T_R = 940 °C

species	L/min	mol/min	mol fraction	g/min	mass fraction	kg/s
O_2	7.83	0.35	0.21	11.18	0.23	1.86×10^{-4}
N_2	29.44	1.31	0.79	36.80	0.77	6.13×10^{-4}
total	37.27	1.66	1	47.98	1	8.0×10^{-4}

Table A4. Boundary Conditions for Urea Solution at NSR = 1.0 in the Case of T_R = 940 °C

species	mol/min	mol fraction	g/min	mass fraction	kg/s
urea	1.33×10^{-2}		0.80		
H_2O	2.18	0.988	39.20	0.980	6.53×10^{-4}
HNCO	1.33×10^{-2}	0.006	0.57	0.014	9.54×10^{-6}
NH_3	1.33×10^{-2}	0.006	0.23	5.66×10^{-3}	3.77×10^{-6}
total	2.20	1	40	1	6.67×10^{-4}

scale reactor. The mass fraction of each species and the total mass flow rate are the values used to input into the CFD code. The wall boundary temperature decreases linearly along the reactor. For example, linear functions of the wall boundary temperatures (T_{wall}) are specified in the case of T_R = 976 °C and NSR = 1.5 and T_R = 980 °C and NSR = 2.0 for each zone of the reactor as follows:

$$T_{wall,I}(x_I) = 727 - 67x_I \text{ (°C)} \quad \text{for } 0 \le x_I \le 1.5 \text{ m} \quad \text{(A2.3)}$$

$$T_{\text{wall,II}}(x_{\text{II}}) = 627 - 250x_{\text{II}}\ (^{\circ}\text{C}) \quad \text{for } 0 \le x_{\text{II}} \le 0.4\ \text{m} \tag{A2.4}$$

$$T_{\text{wall,III}}(x_{\text{III}}) = 527 - 40x_{\text{III}}\ (^{\circ}\text{C}) \quad \text{for } 0 \le x_{\text{III}} \le 2.2\ \text{m} \tag{A2.5}$$

where x (m) is the length along each zone in the reactor. The temperature decreasing rate (250 °C/m) with the length (x) of zone II is highest among zones I, II, and III because of the urea solution injection in this zone.

A3. Governing Equation of Chemical Species (Species Transport Equation). Besides the conservation equations of mass, momentum, and energy, the local mass fraction of each species (Y_i) through the following convection−diffusion equation (or species conservation equation) is solved

$$\frac{\partial}{\partial t}(\rho Y_i) + \nabla(\rho \vec{v} Y_i) = -\nabla \vec{J}_i + R_i + S_i \tag{A3.1}$$

where ρ is the fluid density, $\vec{v}$ is the velocity vector, R_i is the net rate of production of species i by chemical reaction, and S_i is the source term by addition from the dispersed phase, for example, mass addition rate by the droplet evaporation injected from the nozzle (see eq A6.2). $\vec{J}_i$ is the diffusion flux of species i, which arises as a result of concentration gradients. In turbulent flows, the diffusion flux of species i is computed in the following form:

$$\vec{J}_i = -\left(\rho D_{i,\text{m}} + \frac{\mu_{\text{t}}}{\text{Sc}_{\text{t}}}\right)\nabla Y_i \tag{A3.2}$$

where $D_{i,\text{m}}$ is the molecular diffusivity of species i, Sc_{t} is the turbulent Schmidt number ($=\mu_{\text{t}}/\rho D_{\text{t}}$, where μ_{t} is the turbulent viscosity and D_{t} is the turbulent diffusivity). Sc_{t} is set to 0.7 for air.In this study, 13 species (NO, NH_3, HNCO, CO, NCO, N_2O, H_2O, CO_2, O_2, N_2, H, O, and OH) are considered. The time derivative term ($\partial/\partial t(\rho Y_i)$) in eq A3.1 is zero, because all models considered are solved as a steady-state condition. Hereafter, the time-dependent terms are not presented in this CFD model.By integrating the chemical kinetic model with the fluid dynamics, each computational cell in the domain is treated as a continuously stirred tank reactor (CSTR). Each cell may differ from its neighbors with respect to temperature and species concentrations. This allows for a more accurate representation of the chemical reactions occurring in the SNCR process.[19] The chemical reaction rate (R_i) in the present study is modeled in the framework of EDC and is discussed in Appendix A5.

A4. Turbulence Model. One of the simplest models of turbulence in CFD is the standard $k-\varepsilon$ model[26] (two-equation model), in which the solution of two separated transport equations allows for the turbulent velocity and length scales to be independently determined. The model is a semi-empirical model based on model transport equations for the turbulence kinetic energy (k) and its dissipation rate (ε). The model transport equation for k is derived from the exact equation, while the model transport equation for ε is obtained using physical reasoning.The turbulence kinetic energy (k) and its rate of dissipation (ε) are obtained from the following transport equations:

$$\nabla(\rho k u_i) = \nabla\left[\left(\mu + \frac{\mu_{\text{t}}}{\sigma_{\text{k}}}\right)\nabla k\right] + G_{\text{k}} + G_{\text{b}} - \rho\varepsilon \tag{A4.1}$$

$$\nabla(\rho \varepsilon u_i) = \nabla\left[\left(\mu + \frac{\mu_{\text{t}}}{\sigma_{\varepsilon}}\right)\nabla \varepsilon\right] + C_{1\varepsilon}\frac{\varepsilon}{k}G_{\text{k}} - C_{2\varepsilon}\rho\frac{\varepsilon^2}{k} \tag{A4.2}$$

where G_{k} is the generation of turbulence kinetic energy because of the mean velocity gradients and G_{b} is the generation of turbulence kinetic energy because of buoyancy. $C_{1\varepsilon}$ and $C_{2\varepsilon}$ are constants. σ_{k} and σ_{ε} are the turbulent Prandtl numbers for k and ε, respectively. The turbulent (or eddy) viscosity (μ_{t}) is computed by combining k and ε as follows:

$$\mu_{\text{t}} = \rho C_{\mu}\frac{k^2}{\varepsilon} \tag{A4.3}$$

where C_{μ} is a constant. The values used in this study are

$$C_{1\varepsilon} = 1.44,\ C_{2\varepsilon} = 1.92,\ C_{\mu} = 0.09,\ \sigma_k = 1.0,\ \text{and } \sigma_{\varepsilon} = 1.3 \tag{A4.4}$$

which are determined from experiments with air and water for fundamental turbulent shear flows.[26] The turbulence intensity (I) is defined as the ratio of the root-mean-square of the velocity fluctuations (u') to the mean flow velocity (u_{avg}). The turbulence intensity at the core of a fully developed duct flow can be estimated from the following formula derived from an empirical correlation for pipe flows:[25]

$$I \equiv \frac{\sqrt{(u')^2}}{\sqrt{u_{\text{avg}}^2}} = 0.16(\text{Re})^{-1/8} \tag{A4.5}$$

For internal flows, such as a duct flow, the turbulence intensity at the inlets is totally dependent upon the upstream history of the flow.[13,25] In this simulation, the turbulence intensities at the boundary conditions of the reactor and the nozzle inlets are set to 10% by empirical approximation from eq A4.5.

A5. EDC Model for Turbulent Reacting Flow Modeling. All mixing and reaction interaction models impose a number of difficulties in coupling chemistry with CFD codes because they all relate the chemical progress term to one or two parameters from the turbulence modeling.[5] Because the rate of reaction associated with the SNCR chemistry is the same order of magnitude as the rates of turbulent mixing, the effects of turbulence can have a significant effect on the mean rates of the chemical reaction.[1] To consider the turbulent reacting CFD with multistep chemical reactions, the EDC is used for the CFD simulation of SNCR.[5,14,25] The EDC model is an extension of the eddy-dissipation model to include a detailed chemical mechanism in turbulent flow.[27] The principle idea of the EDC is that a turbulent reacting flow can be divided into two parts: fine structures and surrounding fluid.[14] All homogeneous reactions having more than one reactant and thus subject to the mixing process are assumed to take place

Table A5. Boundary Conditions for Urea Solution at NSR = 1.5 in the Case of T_{R} = 940 °C

species	mol/min	mol fraction	g/min	mass fraction	kg/s
urea	1.96×10^{-2}		1.18		
H_2O	2.16	0.982	38.82	0.971	6.47×10^{-4}
HNCO	1.96×10^{-2}	0.009	0.84	0.021	1.41×10^{-5}
NH_3	1.96×10^{-2}	0.009	0.33	8.34×10^{-3}	5.56×10^{-6}
total	2.20	1	40	1	6.67×10^{-4}

Table A6. Boundary Conditions for Urea Solution at NSR = 2.0 in the Case of T_{R} = 940 °C

species	mol/min	mol fraction	g/min	mass fraction	kg/s
urea	2.66×10^{-2}		1.60		
H_2O	2.13	0.976	38.40	0.960	6.40×10^{-4}
HNCO	2.66×10^{-2}	0.012	1.14	0.029	1.91×10^{-5}
NH_3	2.66×10^{-2}	0.012	0.45	1.13×10^{-2}	7.54×10^{-6}
total	2.19	1	40	1	6.67×10^{-4}

(25) Fluent user guide. Fluent 6.3 Documentation, Fluent, Inc., Lebanon, NH, 2007.
(26) Launder, B. E.; Spalding, D. B. *Lectures in Mathematical Models of Turbulence*; Academic Press: London, U.K., 1972.
(27) Magnussen, M. F. The 19th AIAA Meeting, St. Louis, MO, 1981.

Table A7. Reduced Kinetic Parameters Proposed in This Study[a]

number	reaction	pre-exponent (A) [1/(s K^b) or m^3/(s K^b kmol)]	temperature exponent (b)	activation energy (E_a) (J/kmol)
1	$NH_3+NO\rightarrow N_2+H_2O+H$	2.13×10^1 (4.24×10^5)[b]	5.3 (5.3)	2.43×10^8 (3.5×10^8)
2	$NH_3+O_2\rightarrow NO+H_2O+H$	8.83×10^3 (3.50×10^2)	7.65 (7.65)	5.86×10^8 (5.24×10^8)
3	$HNCO+M\rightarrow H+NCO+M$	1.39×10^{13} (2.40×10^{14})	0.85 (0.85)	3.45×10^8 (2.85×10^8)
4	$NCO+NO\rightarrow N_2O+CO$	2.26×10^{15} (1.00×10^{10})	0.0 (0.0)	-2.60×10^7 (-1.63×10^6)
5	$NCO+OH\rightarrow NO+CO+H$	3.68×10^9 (1.00×10^{13})	0.0 (0.0)	0.0 (0.0)
6	$N_2O+OH\rightarrow N_2+O_2+H$	8.60×10^4 (2.00×10^{12})	0.0 (0.0)	8.37×10^7 (4.19×10^7)
7	$N_2O+M\rightarrow N_2+O+M$	8.50×10^7 (1.60×10^{14})	0.0 (0.0)	3.39×10^8 (2.16×10^8)

[a] M is an unknown inert component, and it is not involved in the reduced kinetic mechanism. [b] Kinetic parameters of Brouwer et al.[16]

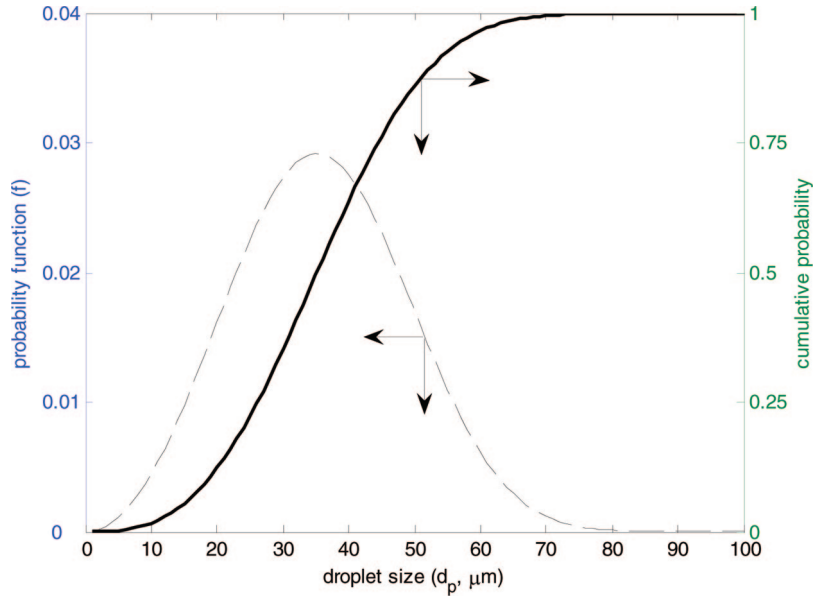

Figure A2. Droplet size probability function of Rosin−Rammler and its cumulative probability within the range of $1 \leq d_p \leq 100$ μm.

only in the fine structures, which are locally treated as well-stirred reactors to transfer mass and energy to the surrounding fluid. The length fraction (or mass fraction) of the fine structures modeled as reported by Gran and Magnussen[28] is

$$\xi^* = C_\xi \left(\frac{\upsilon\varepsilon}{k_i^2}\right)^{1/4} \tag{A5.1}$$

where $*$ denotes the fine structure quantities, C_ξ is the length fraction constant (=2.1377), ν is the dynamic viscosity, and ε is the dissipation rate of turbulent kinetic energy. The volume fraction of the fine structures is calculated as ξ^{*3}. The mean residence time within the fine structures is determined by the dissipation of turbulent kinetic energy (ε) and the dynamic viscosity (ν)

$$\tau^* = C_\tau \left(\frac{\upsilon}{\varepsilon}\right)^{1/2} \tag{A5.2}$$

where C_τ is the time scale constant (by default, $C_\tau = 0.4083$). Elementary reactions proceed over the time scale τ^*, governed by the Arrhenius rate of equations (k_i)

$$k_i = A_i T^b e^{-E_{a,i}/RT}, \quad i = 1, 2, ..., 7 \tag{A5.3}$$

where A_i is the pre-exponential factor for the species i, b is the temperature exponent, E_a is the activation energy (J/kmol), and R is the gas constant (=8314.4 J kmol^{-1} K^{-1}). The reaction kinetic parameters for the seven-step global rate equations are given in Table A7. Those reduced kinetic parameters are estimated at 11% excess oxygen, ignoring the CO concentration. A simplex algorithm in Matlab (fminsearch) is used for parameter estimation in minimizing the square error sum of the NO, NH_3, HNCO, and N_2O concentrations between the full model[15] and the reduced one. The values within the parentheses are referred to in Brouwer et al.[16] For example, the elementary reaction rates are given for NH_3 and NO from Table A7

$$\begin{aligned} r_1 &\equiv \frac{d[NH_3]}{dt} = -k_1[NH_3][NO] - k_2[NH_3][O_2] \\ r_2 &\equiv \frac{d[NO]}{dt} = -k_1[NH_3][NO] + k_2[NH_3][O_2] - \\ &\qquad k_4[NCO][NO] + k_5[NCO] \end{aligned} \tag{A5.4}$$

where the OH radical concentration does not affect the overall SNCR kinetics, assuming that the OH concentration reaches an equilibrium.[16] These reaction rate equations including eq A5.4 are integrated numerically using the ISAT algorithm[29] in the EDC model.The net rate of production of species i by chemical kinetics (R_i) in eq A3.1 is calculated from the mass balance for the fine structure:

$$R_i = \frac{\rho^*(\xi^*)^2}{\tau^*[1-(\xi^*)^3]}(Y_i^* - Y_i) \tag{A5.5}$$

where Y_i^* and Y_i are the species mass fractions of the fine structure after reacting over the time (τ^*) and the surrounding fluid, respectively. ρ^* is the density of the fine structure. The species mass fraction (Y_i^*) is obtained by integrating the elementary reaction rate equations, as mentioned above. The EDC model can

(28) Gran, I. R.; Magnussen, B. F. *Combust. Sci. Technol.* **1996**, *119*, 191–201.

(29) Pope, S. B. *Combust. Theory and Modell.* **1997**, *1*, 41–63.

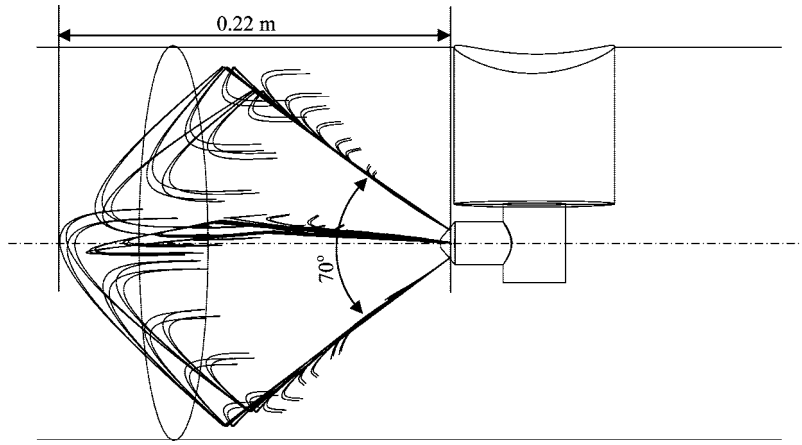

Figure A3. Trajectories of droplets between 1 and 100 μm.

be invariably stiff because of chemical reactions and is computationally expensive.[25]

A6. Droplet Governing Equations. When the urea−water solution is sprayed into the hot flue gas stream, the subsequent reagent generation has two steps: (1) evaporation of water from droplets of the urea−water solution and (2) thermal decomposition of urea into ammonia and isocyanic acid.[30] It is assumed that there is a fast decomposition of urea after evaporation, because the SNCR is operated above 800 °C.[1] The following describes the governing equation for droplets atomized from the nozzle, which includes the momentum, mass, and energy balances. The droplet from the urea−water solution is assumed to be the water droplet, because the dilute urea solution (5 wt %) is used.

A6.1. Droplet Force Balance. The trajectory of a discrete droplet phase is predicted by integrating the force balance on the droplet, which is written in a Lagrangian reference frame. This force balance equates the particle inertia with the forces acting on the particle and can be written for the x and y directions in Cartesian coordinates:[25]

$$\frac{\mathrm{d}u_\mathrm{p}}{\mathrm{d}t} = F_\mathrm{D}(u - u_\mathrm{p}) + \frac{g_x(\rho_\mathrm{p} - \rho)}{\rho_\mathrm{p}} + F_x \qquad \text{(A6.1)}$$

$$\frac{\mathrm{d}v_\mathrm{p}}{\mathrm{d}t} = F_\mathrm{D}(v - v_\mathrm{p}) + \frac{g_y(\rho_\mathrm{p} - \rho)}{\rho_\mathrm{p}} + F_y \qquad \text{(A6.2)}$$

where u and v (m/s) are the gas-phase velocities in the x and y direction, respectively, u_p and v_p (m/s) are the droplet velocities in the x and y direction, respectively, ρ and ρ_p (kg/m^3) are the gas and particle densities, respectively, and $F_\mathrm{D}(u - u_\mathrm{p})$ is the drag force per unit droplet mass defined as

$$F_\mathrm{D} = \frac{18\mu}{\rho_\mathrm{p} d_\mathrm{p}^2}\frac{C_\mathrm{D}\mathrm{Re}_\mathrm{d}}{24} \qquad \text{(A6.3)}$$

where μ (kg/m/s) is the molecular viscosity of the gas phase, d_p is the droplet diameter, and C_D is the drag force coefficient. The relative Reynolds number (Re_d) is defined as

$$\mathrm{Re}_\mathrm{d} = \frac{\rho d_\mathrm{p}|u_\mathrm{p} - u}{\mu} \qquad \text{(A6.4)}$$

F_x and F_y terms in the equations of motion in eqs A6.1 and A6.2 are additional accelerations in the x and y directions, respectively (force/unit particle mass). The additional accelerations are the force to accelerate the gas surrounding the droplet. This force can be written for the x and y directions

$$F_x = \frac{1}{2}\frac{\rho}{\rho_\mathrm{p}}\frac{\mathrm{d}}{\mathrm{d}t}(u - u_\mathrm{p}) \qquad \text{(A6.5)}$$

$$F_y = \frac{1}{2}\frac{\rho}{\rho_\mathrm{p}}\frac{\mathrm{d}}{\mathrm{d}t}(v - v_\mathrm{p}) \qquad \text{(A6.6)}$$

It is found in the CFD simulation with the droplet model that the velocity of the droplets at the nozzle tip is about 25 m/s. The probability density function of Rosin−Rammler[24] is used to represent a non-uniform droplet size

$$f(d_\mathrm{p}) = q\frac{d_\mathrm{p}^{\,q-1}}{X^q}\exp\left[-\left(\frac{d_\mathrm{p}}{X}\right)^q\right] \qquad \text{(A6.7)}$$

$$X = \frac{d_\mathrm{p,mean}}{\Gamma(1/q + 1)} \qquad \text{(A6.8)}$$

where q (=3.0) is the dimensionless dispersion coefficient, $d_\mathrm{p,mean}$ (=36 μm) is the arithmetic mean diameter of the droplets, and Γ is the Gamma function. Figure A2 shows the droplet size distribution function (f) and the cumulative probability according to the droplet size (d_p) between 1 and 100 μm.

The trajectory and velocity profile of the droplets are plotted in Figure A3. The maximum penetration length of the biggest droplets (100 μm) is about 0.22 m, and the injection angle of 70° is formed from the six holes on the nozzle tip.

A6.2. Law of Droplet Boiling. The droplets disappear according to the following three steps: inert heating, evaporation, and boiling. Because the urea solution is injected from the nozzle tip at 100 °C, which is the boiling point of water, the droplets undergo only the boiling step.

The droplet boiling law is used to predict the boiling of a discrete phase droplet when the droplet temperature (T_p) reached the boiling point (T_bp)[25]

$$T_\mathrm{p} \geq T_\mathrm{bp} \qquad \text{(A6.9)}$$

$$m_\mathrm{p} > (1 - f_\mathrm{v})m_\mathrm{p,0} \qquad \text{(A6.10)}$$

where m_p (kg) is the mass of the droplet particle, $m_\mathrm{p,0}$ (kg) is the initial mass of the droplet, and f_v is the volatile fraction.

The boiling rate equation (or evaporation rate and droplet mass balance)[30,31]is expressed as follows:

(30) Birkhold, F.; Meingast, U.; Wassermann, P.; Deutschmann, O. *Appl. Catal., B* **2007**, *70* (1−4), 119–127.

(31) Abramzon, B.; Sirignano, W. A. *Int. J. Heat Mass Transfer* **1989**, *32* (9), 1605–1618.

$$\frac{d(m_p)}{dt} \equiv 0 = \frac{4k_\infty}{\rho_p c_p d_p}(1 + 0.23\sqrt{Re_d})\ln\left[1 + \frac{c_{p,\infty}(T_\infty - T)}{h_{fg}}\right] \quad \text{(A6.11)}$$

where c_p (=4.182 J kg^{-1} K^{-1}) is the specific heat capacity of the droplet, k_∞ (= 0.6 W m^{-1} K^{-1}) is the thermal conductivity of the gas, $c_{p,\infty}$ (J kg^{-1} K^{-1}) is the heat capacity of the gas, T_∞ is the local temperature of the continuous phase, and h_{fg} (=2.263 MJ/kg) is the latent heat of water.

EF8004652